Buffer-Gas Cooled Bose-Einstein Condensate

S. Charles Doret,[1,3] Colin B. Connolly,[1,3] Wolfgang Ketterle,[2,3] and John M. Doyle[1,3]

[1]*Department of Physics, Harvard University, Cambridge, Massachusetts 02138, USA*
[2]*Department of Physics, MIT, Cambridge, Massachusetts 02139, USA*
[3]*Harvard-MIT Center for Ultracold Atoms, Cambridge, Massachusetts 02138, USA*

We report the creation of a Bose-Einstein condensate using buffer-gas cooling, the first realization of Bose-Einstein condensation using a broadly general method which relies neither on laser cooling nor unique atom-surface properties. Metastable helium (^{4}He*) is buffer-gas cooled, magnetically trapped, and evaporatively cooled to quantum degeneracy. 10^{11} atoms are initially trapped, leading to Bose-Einstein condensation at a critical temperature of 5 μK and threshold atom number of 1.1×10^6. This method is applicable to a wide array of paramagnetic atoms and molecules, many of which are impractical to laser cool and impossible to surface cool.

Now well into its second decade, the experimental realization of Bose-Einstein condensation (BEC) in dilute gases has led to revolutionary advances in physics. Since this achievement the field has moved quickly, with innumerable new developments in coherent atom and molecular optics and nonlinear atom optics, the observation of superfluidity in atomic gases, the study of novel quantum systems, and most recently the study of the BEC-BCS crossover (see [1–3] and references therein). Despite the breadth of new research, the basic recipe for BEC is unchanged from its first realization in alkali atoms: precool a hot sample utilizing laser cooling to permit trapping and provide high densities, followed by evaporative cooling to reach quantum degeneracy. Research on quantum degenerate gases is critically reliant on this initial laser-cooling step. In this Letter we describe the first creation of a Bose-Einstein condensate using buffer-gas cooling, thereby demonstrating a method for creating quantum gases that is free of both laser cooling and cryogenic surface contact cooling (used uniquely with atomic hydrogen [4]). This circumvents the limitations of these techniques and dramatically expands the palette of atoms and molecules accessible for study in the ultracold regime.

Experiments with ultracold atoms or molecules all include an initial cooling and trapping stage using one of the three possible methods for cooling: (1) interactions with light, (2) direct contact with a cold surface, or (3) collisions with a gas. Of the three methods, it is laser cooling that has driven the explosive growth of ultracold atom research. Laser cooling has been applied to several atomic species, including the alkalis, alkaline earths, metastable noble gases, and a few others. However, laser cooling can be usefully applied only to atoms with a level structure that permits the practical cycling of many photons at a technologically accessible wavelength. Furthermore, optical absorption and light-induced collisions limit the number and density of atoms that may be cooled [5]. Though recent

proposals show the possibility of laser cooling certain molecules [6,7], no molecules have yet been directly laser cooled due to their complex structure, limiting study of ultracold molecular species to those which may be assembled from laser cooled atoms via Feshbach resonances or photoassociation. A possible alternative approach, surface contact cooling, suffers from the strong constraint of rapidly declining vapor pressures at low temperatures. This limits its use for trapping experiments to only a single species, atomic hydrogen (^{1}H); all other atoms or molecules strongly adsorb onto surfaces at the low temperatures required for trapping [8]. It is thus important to develop new cooling techniques applicable to a wide range of new atoms as well as molecules to take full advantage of scientific opportunities in new areas. Buffer-gas cooling is one such approach.

Buffer-gas cooling is an implementation of cooling via collisions with a gas. In contrast with laser cooling, buffer-gas cooling relies only on elastic collisions between a species of interest and a cryogenic helium buffer gas to cool a sample [9]. This makes it largely independent of the details of the species in question, circumventing all of the limitations of laser cooling and surface contact cooling (as described above). Buffer-gas cooling can in principle be used to trap large numbers of a wide array of paramagnetic atoms (about half of the periodic table), as well as some molecules. Which of the candidates have a sufficiently favorable ratio of elastic to inelastic collisions for evaporative cooling is the subject of ongoing research [10,11]. Earlier work has demonstrated the trapping of Eu, Cr, Mo, Dy, Ho, Nd, Pr, Tb, Au, Ag, Cu, Mn, Li, Na, N, and even the molecular species CaH, NH, CrH, and MnH [9]. Trapping of large numbers (several orders of magnitude larger than samples trapped by laser cooling) gives buffer-gas cooling the potential to produce correspondingly larger condensates containing 10^9 or more atoms, create very large reservoirs of ultracold atoms for use as a sympathetic

103005-1

coolant, and provide a source for creation of ultracold molecules of new and varied elemental composition. Despite the generality and potential advantages of buffer-gas cooling, it has not previously been used to create a quantum degenerate gas.

In this work we present a new realization of BEC in ^{4}He* based on buffer-gas cooling, the first Bose-Einstein condensate created using this general cooling technique. Although we could have chosen from a wide variety of new atomic species, we selected ^{4}He* for our demonstration since it has been previously condensed [12–15] (using laser precooling), ensuring that the ultracold collisional properties of the species allow for a stable condensate. Bose condensation of any paramagnetic species with collisional parameters that allow for efficient evaporative cooling (see [16]) may be achieved with changes only to the production and detection aspects of this experiment.

The apparatus, shown in Fig. 1, is an improvement upon that described in Ref. [17]. A double-walled plastic cell is maintained at 200 mK by a superfluid helium heatlink to a dilution refrigerator. The cell resides inside the bore of a large superconducting anti-Helmholtz magnet which generates a spherical quadrupole field with trap depths as great as 3.7 T (5 K for He*). This electrically insulating cell enables rapid changes of magnetic fields and also permits the introduction of radio-frequency (rf) fields for the production of ^{4}He* and for rf-induced evaporation. The cell is divided into two chambers by a cryogenic valve: a lower chamber where ^{4}He* is produced and trapped and an upper pumping chamber with an activated charcoal sorb. The trapping chamber has an extension to provide space for a

FIG. 1 (color).   Schematic of the experimental apparatus.

second set of superconducting magnets that produce a quadrupole-Ioffe configuration (QUIC) trap [18].

^{4}He* atoms are produced via rf discharge in a method described in detail in Ref. [17]. Briefly, a thin helium film is desorbed from the walls using a pulsed laser, producing a buffer gas, and a small fraction ($\sim 10^{-5}$) is converted from ^{4}He to ^{4}He* by a 200 μs rf discharge pulse. The ^{4}He* is cooled to ~ 500 mK by collisions with the buffer gas and trapped, and the buffer gas is cryopumped to the cell walls and charcoal sorb in about 1 ms, providing excellent vacuum and lifetimes limited only by Majorana loss. Approximately 10^{11} atoms are trapped in the fully stretched state $|S = 1, m_S = +1\rangle$ at peak densities of 10^{12} cm^{-3}.

Reducing currents in the anti-Helmholtz coils drives forced evaporative cooling, as atoms striking any wall are de-excited and adsorbed. The trap depth is initially equal along the cell's circumference and at the top of the narrow extension to the trapping chamber (see Fig. 1). After an initial period of uniform lowering we reduce the current in only the bottom coil, causing evaporation against the extension as the trap minimum shifts towards it. This asymmetric reduction maintains field gradients while reducing the trap depth, increasing the density and collision rate in the atom cloud during cooling. Currents are reduced over 100 s from 100 A to 10 and 3 A in the top and bottom coils, respectively, with ramp rates set by power supply limitations rather than ^{4}He* collision rates. This shifts the cloud completely into the extension, cooling the atoms to roughly 2 mK with approximately 5×10^8 atoms remaining.

As the atoms are cooled the Majorana lifetime drops from hundreds of seconds to about 30 s. Further evaporation in the quadrupole field continues to shorten the lifetime, necessitating a switch to an Ioffe-Pritchard trapping geometry. We use a set of three additional superconducting coils: a small quadrupole pair with winding directions matching the large trapping magnet and a third (Ioffe) coil oriented perpendicular to the cell axis [19]. With 6.4 A in the quadrupole pair and 17 A in the Ioffe coil we form a QUIC trap with radial gradient 380 G/cm, axial curvature 625 G/cm^2, and 1.6 G bias. This corresponds to $\omega_z = 2\pi \times 210 \pm 10$ Hz (measured by modulating trap currents and observing atom loss) and $\omega_r = 2\pi \times 2520 \pm 240$ Hz (inferred from the aspect ratio of trapped atom clouds). The quadrupole coils are located such that the QUIC trap minimum is roughly aligned with the cell axis. Currents are capacitively filtered and actively stabilized to the 10^{-5} level to reduce field noise and bias drift. Simultaneously ramping down the anti-Helmholtz trap while ramping up the QUIC currents allows smooth transfer of atoms into the QUIC trap. We perform this transfer in 5 seconds, limited by highly inductive anti-Helmholtz coils. Transfer efficiencies of nearly 100% should be possible [18], but are presently limited to 10% by skimming of warm atoms out of the trap due to geometric constraints
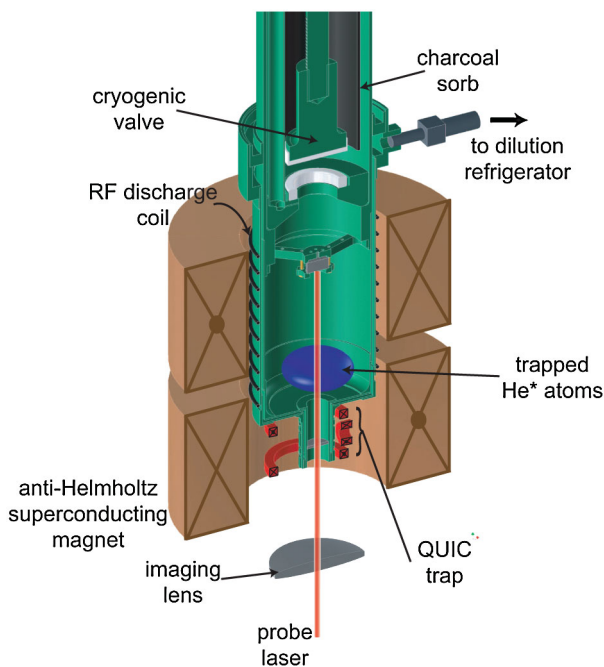
associated with retrofitting the QUIC trap into an existing apparatus. After transfer to the QUIC trap one-body lifetimes exceed 10 minutes; two-body processes limit lifetimes for densities of $\sim 10^{11}$ cm^{-3} or greater.

After transfer to the QUIC trap 5×10^7 atoms remain, now at a temperature of 500 μK due to the aforementioned skimming. Further cooling is accomplished via rf-induced evaporation, as the atoms are now cold and slow enough to use moderate rf powers and low frequencies. Radio frequency is introduced to the cell via superconducting Helmholtz windings around the cell extension. This produces a $\vec{B}$ field perpendicular to the QUIC trap bias field, permitting good coupling to the atom cloud. 5 dBm of rf is applied for ~ 12 seconds in a piecewise linear ramp (somewhat faster than exponential) beginning at 140 MHz. Faster and slower ramps also produce a condensate, but suffer from rf power limitations or collisional losses upon condensate formation, respectively.

Detection is accomplished by imaging the cloud onto a CCD camera (quantum efficiency (QE) $\sim 1\%$ at 1083 nm), both *in situ* and in time of flight (TOF). To mitigate the low saturation intensity of the imaging transition, photon recoil-induced blurring, low camera QE, and losses from dewar optics, phase-contrast imaging [20] is used to permit far-detuned imaging at larger intensities. Limited resolution precludes *in situ* observation of the radial dimension of the coldest clouds, so at temperatures below 20 μK we detect in TOF expansion by rapidly shutting off the QUIC trap. Expansion times of $t_{\text{expand}} < 1.5$ ms are chosen to keep the optical density large enough to permit far-detuned imaging and minimize effects from currents induced by trap turn-off.

When the final rf frequency of the evaporative cooling ramp is lowered to within 1.05 MHz of the trap bottom, we observe the formation of a Bose-Einstein condensate as the onset of a bimodal structure to the spatial distribution of the expanded cloud, characterized by a broad spherical region surrounding a narrow elliptical core (see Fig. 2). As the rf frequency is swept to lower values the intensity of the Bose-condensed core is strengthened at the expense of the surrounding spherical thermal cloud, as in Fig. 3. Lowering the rf frequency below 0.3 MHz above the trap bottom produces a nearly pure condensate. Figure 4 demonstrates the sudden onset of these changes to the TOF distribution, as manifested by a dramatic shrinking of the effective cloud area below 1.05 MHz.

The temperature, T_c, and atom number, N_c, at the transition point are each determined in two ways. Fits to radial profiles of TOF images indicate $T_c = 4.5 \pm 0.5$ μK, but suffer from uncertainty as to whether QUIC trap turn-off is truly sudden. An independent estimate is made using the measured ratio η between the trap depth and atom temperature observed *in situ* at higher temperatures and the trap depth at T_c; this implies a critical temperature of 5 μK. A critical atom number of $N_c = 2 \times 10^6$ is determined by integrating over phase-contrast images taken in TOF. However, uncertainties in laser detuning (due to induced currents) and possible saturation effects as well as the sensitivity of phase-contrast images to imaging system details make this number accurate only to within a factor of 2. Alternatively, assuming an ideal Bose gas one can use T_c to calculate $N_c = 1.202(k_B T/\hbar\omega_r^2\omega_z)$, giving $N_c = 1.1 \pm 0.4 \times 10^6$ and indicating a peak density of 2.2×10^{13} cm^{-3}. Generally 20% of these atoms are cooled into a nearly pure condensate with lifetimes of approximately 1 s, presumably limited by Penning ionization [14]. Significant improvements to these numbers should be attainable with straightforward modifications to the experiment, including increasing transfer efficiency between anti-Helmholtz and QUIC trapping geometries and increasing initial ^{4}He* production. Future work with ^{3}He*/^{4}He* mixtures is also a direct extension.

In conclusion, we have achieved BEC in ^{4}He* using buffer-gas cooling, the first demonstration of a general
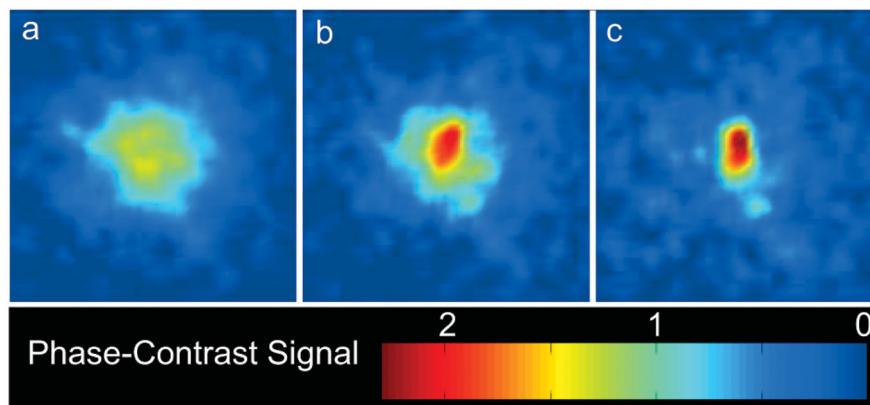

FIG. 2 (color).   Two-dimensional phase-contrast images after 1 ms TOF showing the onset of BEC. Each panel is the average of three individual clouds. (a) An approximately spherical thermal cloud slightly above T_c. (b) Just below T_c the condensate appears in the center of the image, characterized by a larger density and elliptical shape. (c) A nearly pure condensate after further evaporative cooling. Field of view is 600 μm, and laser detuning is $7.5 \times \Gamma/2$, where $\Gamma = 1.6$ MHz is the natural linewidth.
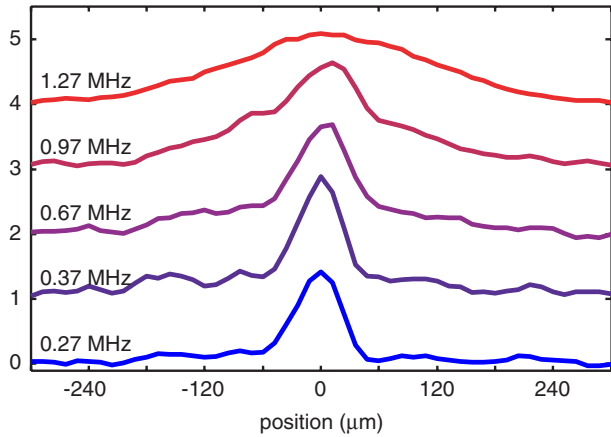
FIG. 3 (color online).   Phase-contrast signal of cross sections along the axial dimension after 1 ms TOF for varying values of the final rf evaporation frequency. Each trace is an average over three runs of the experiment. For values of $\nu_{rf} < 1.05$ MHz the cross sections show the bimodal distribution characterizing the presence of both thermal and Bose-condensed components. The top four cross sections are offset vertically for clarity. Laser detuning is $7.5 \times \Gamma/2$.

method for producing quantum degenerate gases not relying on laser cooling or surface contact cooling for initial trap loading. This makes possible new research on ultracold gases with a wide array of atoms and molecules not previously accessible. Ultracold molecules, in particular, present a wealth of opportunities for quantum computation [21,22] and precision measurement [23], while highly magnetic atoms are candidates for new dipolar gases and
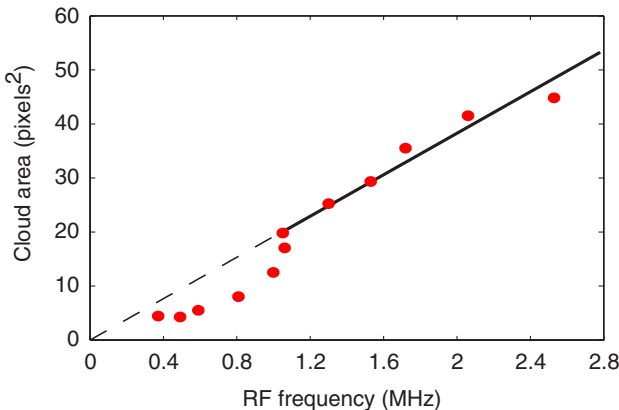

FIG. 4 (color online).   Cloud area in TOF as a function of ν_{rf}, measured as $\sigma_x \times \sigma_y$ of a two-dimensional Gaussian fit. Pixels are 12 μm square. Atom temperature varies approximately linearly with rf frequency; for $T > T_c$ the area follows the classical result and is proportional to temperature. The sudden change at $\nu_{rf} = 1.05$ MHz signals the appearance of the condensate; below this frequency clouds no longer fit well to a single Gaussian, requiring different widths for the condensate and thermal fraction. A systematic error of 0.07 MHz from possible QUIC bias field drift affects all data.

searches for time variation of fundamental constants [24]. The addition of optical potentials—feasible in a similar apparatus—further expands the opportunities available. Buffer-gas cooling shall also enable creation of bosonic and fermionic gases of unprecedented size for hydrodynamic studies and sympathetic cooling. Finally, quantum degenerate gases in new species provide a laboratory for collisional studies and may open the door to unforeseen and interesting new physics.

[1]   J. R. Anglin and W. Ketterle, Nature (London) **416**, 211 (2002).
[2]   J. D. Weinstein *et al.*, Phys. Rev. A **57**, R3173 (1998).
[3]   I. Bloch, J. Dalibard, and W. Zwerger, Rev. Mod. Phys. **80**, 885 (2008).
[4]   D. G. Fried *et al.*, Phys. Rev. Lett. **81**, 3811 (1998).
[5]   W. Ketterle *et al.*, Phys. Rev. Lett. **70**, 2253 (1993).
[6]   B. K. Stuhl *et al.*, Phys. Rev. Lett. **101**, 243002 (2008).
[7]   M. D. DiRosa, Eur. Phys. J. D **31**, 395 (2004).
[8]   J. M. Doyle, Ph.D. thesis, M. I. T., (1991).
[9]   W. Campbell and J. Doyle, *Cold Molecules: Theory, Experiment, Applications* (Taylor and Francis, Boca Raton, 2009), Chap. 13, p. 473.
[10] C. B. Connolly *et al.* (to be published).
[11] M.-J. Lu, V. Singh, and J. D. Weinstein, Phys. Rev. A **79**, 050702(R) (2009).
[12] A. Robert *et al.*, Science **292**, 461 (2001).
[13] F. Pereira Dos Santos *et al.*, Phys. Rev. Lett. **86**, 3459 (2001).
[14] A. S. Tychkov *et al.*, Phys. Rev. A **73**, 031603(R) (2006).
[15] R. G. Dall and A. G. Truscott, Opt. Commun. **270**, 255 (2007).
[16] W. Ketterle and N. J. van Druten, Adv. At. Mol. Opt. Phys. **37**, 181 (1996).
[17] S. V. Nguyen *et al.*, Phys. Rev. A **72**, 060703(R) (2005).
[18] T. Esslinger, I. Bloch, and T. W. Hansch, Phys. Rev. A **58**, R2664 (1998).
[19] Quadrupole coils: $R_{inner} = 18.4$ mm, $R_{outer} = 23.4$ mm, $L = 5$ mm, 430 turns; Ioffe coil: $R_{inner} = 3$ mm, $R_{outer} = 6.8$ mm, $L = 6.3$ mm, 410 turns.
[20] W. Ketterle, D. Durfee, and D. Stamper-Kurn, *Bose-Einstein Condensation in Atomic Gases* (IOS Press, Amsterdam, 1999), pp. 67–176.
[21] D. DeMille, Phys. Rev. Lett. **88**, 067901 (2002).
[22] P. Rabl *et al.*, Phys. Rev. Lett. **97**, 033003 (2006).
[23] M. Kozlov and L. Labzowsky, J. Phys. B **28**, 1933 (1995).
[24] V. A. Dzuba, V. V. Flambaum, and J. K. Webb, Phys. Rev. Lett. **82**, 888 (1999).